

Date 2013
Author Essen, S. van, A. van der Hout, R.H.M. Huijsmans and
O. Waals
Address Delft University of Technology
Ship Hydromechanics and Structures Laboratory
Mekelweg 2, 2628 CD Delft



Delft University of Technology

Evaluation of directional analysis methods for low-frequency waves to predict LNGC motion response in nearshore areas

by

**S. van Essen, A. van der Hout, R.H.M. Huijsmans and
O. Waals**

Report No. 1874-P

2013

**Proceedings of the ASME 2013 32nd International Conference
on Ocean, Offshore and Arctic Engineering, OMAE2013, June 9-14,
2013, Nantes, France, Paper 10235.**

OMAE2013-10235

EVALUATION OF DIRECTIONAL ANALYSIS METHODS FOR LOW-FREQUENCY WAVES TO PREDICT LNGC MOTION RESPONSE IN NEARSHORE AREAS

Sanne van Essen
Deltares, presently MARIN
Delft, The Netherlands

René Huijsmans
Delft University of Technology
Delft, The Netherlands

Arne van der Hout
Deltares
Delft, The Netherlands

Olaf Waals
MARIN
Wageningen, The Netherlands

ABSTRACT

Because LNG terminals are located increasingly close to shore, the importance of shallow-water effects associated with low-frequency (LF) waves increases as well. The LF wave spectrum in these areas is generally complex, with multiple frequency peaks and/or directional peaks due to LF wave interaction with the shore. Both free and bound LF waves at the same frequency can be present. Since LF waves are potentially very significant for moored vessel motions, it is important to include their effect in an early stage of the terminal design. This requires an efficient and relatively simple tool able to estimate the LF wave spectrum in nearshore areas. The benefit of such a procedure with respect to state-of-the-art response methods is the ability to include the LF free wave distribution in a local wave field in the vessel response calculation.

The objectives of the present study are to identify such a tool, and to evaluate the use of its output as input for a vessel motion calculation. Three methods, designed for the determination of wave spectra of free wave-frequency (WF) waves, were applied to artificial LF wave fields for comparison of their performance. Two stochastic methods, EMEP (Hashimoto *et al.*, 1994) and BDM (Hashimoto *et al.*, 1987) and one deterministic method, r-DPRA (De Jong and Borsboom, 2012) were selected for this comparison. The foreseen application is beyond the formal capabilities for which these three methods were intended. However, in this study we have investigated how far we can take these existing methods for the determination of directional LF wave spectra.

Sensitivity analyses showed that the EMEP method is the most suitable method of the three for a range of LF wave fields. The reconstructed LF wave spectra using EMEP resembled the input spectra most closely over the whole range

of water depths and frequencies, although its performance deteriorated with increasing water depth and wave frequency. Subsequently, a first effort was made to use the information in the reconstructed EMEP LF wave spectrum of a representative shallow-water wave field for a first estimate of the motions of a moored LNG carrier. The results were acceptable. This is a first indication that EMEP output might be used to calculate the motions of an LNG carrier moored in shallow water.

1 INTRODUCTION

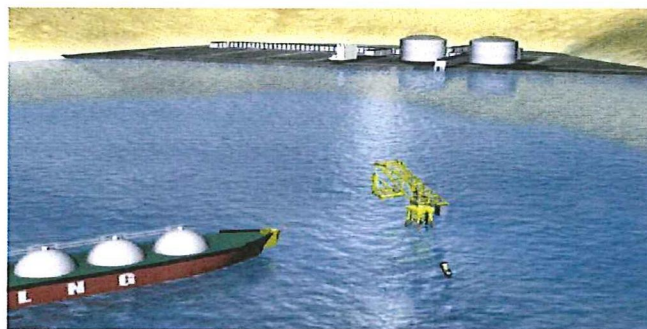


Figure 1 Impression of a nearshore moored LNGC (from [8])

This research project was initiated as a reaction to questions arisen within the sHALLOW Water Initiative Joint Industry Project (HAWAI JIP) and its successor HAWAII [7][8]. This study has been conducted as a spin-off outside the original scope of HAWAII. In recent years, there has been an increased interest in Liquid Natural Gas (LNG) terminals at nearshore locations (15-40m water depth, Figure 1). Hydrodynamic design calculations for LNG carriers (LNGC) usually rely on deep-water wave theory, while experience with

vessels at these nearshore terminals shows that shallow-water effects on LNG carriers can have a high influence on terminal performance. This was the incentive for JIP-HAWAI, which had the objective to improve the reliability of such nearshore LNG terminals.

Both the energy and the directional spreading of low frequency (LF) waves are high in nearshore areas. This is not always accounted for in commonly applied design procedures. The eigenfrequencies of the horizontal motions of a typical moored LNGC are in this LF range (0.3-0.03rad/s). Combined with the low damping characteristics of typical terminal mooring systems, this can lead to large resonant motions and possibly high down-times. An important conclusion drawn from JIP-HAWAI was that LF (free) waves can dominate the overall response of an LNGC in shallow water, which is why LF shallow water waves should be included in shallow-water terminal and vessel design [7]. The main aim of the second JIP was to develop a design methodology for offshore terminals in a nearshore wave climate [8]. In an early stage of such a design procedure, an approach is desired to quickly estimate the response of a vessel to a certain (LF) wave field. This requires a tool, which is able to determine the directional LF wave spectrum (Figure 2). The term ‘wave spectrum analysis’ refers to the procedure used in such a tool. This led to the objectives of the current research project:

1. To identify a suitable existing method, originally designed to analyze free WF waves, for the determination of the directional LF wave spectrum in shallow water.
2. To evaluate whether output from this method forms suitable input for a first estimate of the response of a benchmark LNGC moored at a shallow-water terminal.

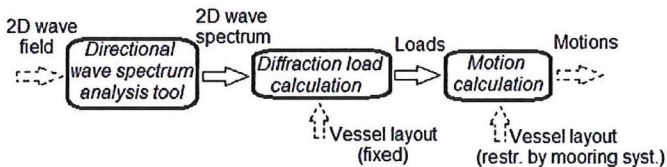


Figure 2 General vessel motion calculation procedure in a preliminary design cycle of a LNGC (terminal)

2 BACKGROUND THEORY

2.1 Wave components in shallow water

Shallow-water wave fields generally consist of first- and second-order wave components. The first-order components can be divided in free WF and LF components, respectively called WF primary and LF free components here. These two types of first-order components can be distinguished by their frequency, and generally by their origin. All first-order wave components travel with a velocity according to the dispersion relation.

The most important second-order phenomenon for a system with a low natural frequency in shallow water is the occurrence of bound waves, which are excited by difference-interactions between first-order components. The variation of wave

amplitude in a wave field induces spatial and temporal variations in radiation stresses, to which the mean water surface responds [17]. A relatively high wave amplitude at some location induces local set-down (a low mean surface elevation); a relatively low wave amplitude has the opposite effect: set-up.

This variation of the mean surface elevation can be seen as an LF wave that is bound to the wave group. Such a second order bound wave under a bichromatic wave signal consisting of two harmonic WF primary waves is shown in Figure 3.

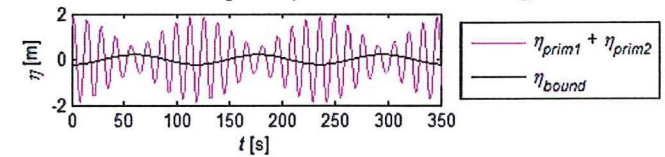


Figure 3 Bound wave excited by a bichromatic pair of primary waves according to [17] – $\omega_1 = 0.51\text{rad/s}$, $\omega_2 = 0.46\text{rad/s}$, water depth $h = 15\text{m}$

A primary wave combination of two waves with frequencies ω_1 and ω_2 excites a bound wave with frequency $\omega_{\text{bound}} = \Delta\omega = \omega_2 - \omega_1$. The velocity of this wave can be deduced from its frequency and wave number, using $c_{\text{bound}} = \omega_{\text{bound}}/k_{\text{bound}}$. The bound wave number follows from the vector sum of the wave numbers of the exciting primary waves, and does not satisfy the dispersion relation: $\bar{k}_{\text{bound}} = \bar{k}_2 - \bar{k}_1$. Many different combinations of primary waves can have the same difference frequency, which leads to different possible bound wave numbers and wave velocities for one difference frequency ω_{bound} [12][25].

LF free waves, which are first-order wave components, can be formed by interaction of bound waves with the shoreline; it was suggested by [17] (based on earlier observations [20][24]) that shoreward propagating bound waves are released as LF free waves after reflecting off the coast and propagate offshore. LF free waves can also originate from distant sources, although the energy content of these waves is generally small compared to the energy of the locally generated waves for more energetic sea states [9].

This means that LF waves in shallow water exist in two forms that travel with different velocities, and possibly in different directions: bound waves excited as secondary effect of primary waves and LF free waves. Components with the bound wave velocity c_{bound} and the free wave velocity c_{free} can be present at the same frequency in such wave fields. It is generally assumed that the total LF energy in shallow water is dominated by bound incident waves and LF free reflected waves and that the bound reflected waves and LF free incident wave can be neglected (e.g. [9][13]).

2.2 The 2D wave spectrum

A 2D wave spectrum describes the distribution of wave energy in a wave field over frequencies and directions. It gives a complete statistical description of the water surface if this surface can be seen as a stationary Gaussian process (e.g. [14]),

assuming that a wave field consists of a superposition of many independent sinusoidal wave contributions [21].

The 2D wave spectrum in this report refers to a variance density spectrum $E(\omega, \theta)$, which describes the distribution of mean variance over wave directions and frequencies (e.g. [2][14]). Variance is defined using the wave amplitude as $\sigma_{nm}^2 = 0.5 a_{nm}^2$. In wave spectrum determination procedures, a 2D wave spectrum $E(\omega, \theta)$ is usually decomposed in a 1D frequency spectrum $E(\omega)$ and a directional spreading function (DSF) $D(\theta)$, describing the variance distribution over the directions (Eq. 1, from [2]).

$$\begin{aligned} E(\omega, \theta) &= E(\omega) D(\theta) \quad \text{with:} \\ D(\theta) &\geq 0 \quad \text{over } [0, 2\pi] \quad \text{and} \quad \int_0^{2\pi} D(\theta) d\theta = 1 \end{aligned} \quad \text{Eq. 1}$$

2.3 Directional wave analysis methods

Including LF wave effects in shallow water in a first estimate of the vessel response requires a wave spectrum analysis tool, that determines the 2D LF wave spectrum of a local wave field. There are many types of 2D wave analysis methods available. Their wave splitting capability is based on the known velocity of each free wave frequency component, according to the dispersion relation. This leads to difficulties if these methods are applied to LF wave fields, because components with c_{bound} and c_{free} can be present at the same frequency in such wave fields (as mentioned in Section 2.1). This means that either these methods have to be adjusted to include bound waves, or this difference is neglected. In the latter case, it should be investigated whether existing methods provide a sufficiently accurate estimate of the LF spectrum.

The first option has only been implemented for 1D wave fields, and extending these methods to 2D is a complicated procedure. Here a '1D wave field' refers to a uni-directional wave field propagating perpendicular to an alongshore uniform coast, where the only possible wave directions are incident and reflected. A '2D wave field' is a wave field where wave components can travel in arbitrary directions. For 1D wave fields, there are methods available that find the energy of each directional component (incoming and reflected), but also tools that distinguish between bound and LF free components [1][27]. These methods use a deterministic least-squares technique to solve the wave system.

All available methods for 2D directional wave spectrum determination are essentially developed for primary WF waves (with shorter wavelengths and wave periods) and assume that all waves are free (the 'free wave assumption'). Stochastic methods are the most commonly used type of 2D wave analysis methods. These methods use a random-phase assumption; they try to find the 2D spectrum of a certain wave field, but lose its phase information. This is something deterministic methods preserve; they attempt to find both the directional spectrum and the phase information. Many different methods are available, especially in the class of stochastic models.

In this study, it was chosen to evaluate existing 2D analysis methods that use the free wave assumption, which might be acceptable because the difference between c_{bound} and c_{free} decreases towards shallow water [4] Figure 4 shows the velocity ratio c_{bound}/c_{free} over water depth domain 15-40m and frequency domain 0.03-0.3rad/s. This figure was generated for an LF free and a bound component at the same frequency ω_{low} , where the bound wave is excited by a bichromatic pair of primary waves with frequencies $\omega_1 = 0.35\text{rad/s}$ and $\omega_2 = \omega_1 + \omega_{low}$. This figure shows that the velocity ratio approaches the value one for shallow water and a low frequency.

A complicating factor is that a high directional spreading in a 2D wave field leads to a ratio of c_{bound}/c_{free} that increases slower to one than of a wave field with a narrow DSF (Figure 5). This means that it is expected that 2D wave analysis with free wave assumption will perform less for wave fields that include bound waves with a high directional spreading.

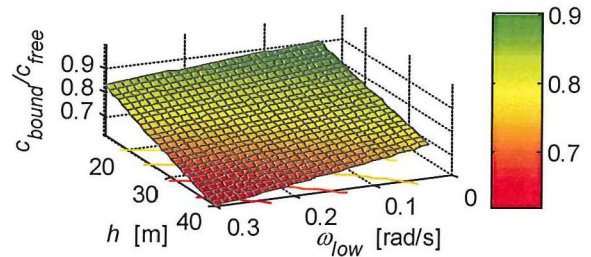


Figure 4 Velocity ratio c_{bound}/c_{free} of 1D free and bound waves at the same ω_{low} for $h = 15\text{-}40\text{m}$ and $\omega_{low} = 0.03\text{-}0.3\text{rad/s}$

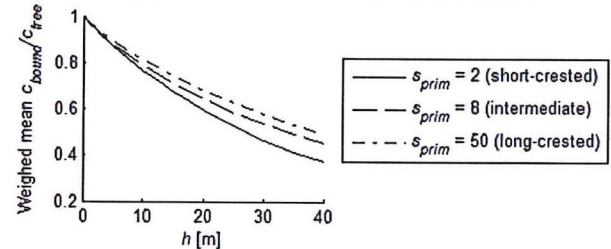


Figure 5 Effect of primary directional spreading parameter s_{prim} on 2D LF velocity ratio c_{bound}/c_{free} towards shallow water

Another difficulty in the analysis of shallow-water LF wave fields is that reflection can cause standing-wave patterns (e.g. edge waves). Such patterns cannot be solved with a method that uses a random-phase assumption, because incident and reflected components in standing waves are phase-locked. It was assumed that these patterns are not dominant for LF waves in the considered water depths, due to the high directional spreading of these waves, their frequency spreading and the occurrence of both bound incident and LF free reflected wave components.

The last difficulty of these nearshore LF wave fields is that a high directional spreading is present. Many directional wave spectrum determination methods use one, or a couple of principle directions, which are used to fit the available

measurements to. This is not sufficient in wave fields with a high directional spreading.

2.4 Vessel motion response calculation methods

2.4.1 Secondary wave drift loads

An important feature of the diffraction methods that are commonly applied to calculate vessel response, is that they use ship-specific transfer functions; linear load response amplitude operators (FRAOs) for the primary loads, and non-linear quadratic transfer functions (QTF) for the secondary drift loads. A QTF entry describes the load on the vessel due the interaction of two primary wave components. Standard diffraction methods use QTFs based on second-order wave drift theory for long-crested¹ waves; they do not account for the interactions of primary wave components traveling in different directions [22]. This QTF version is called '2D-QTF'. An alternative, more advanced way of defining the QTF is to include interactions between wave components in different directions (as found in short-crested seas). This QTF description includes four summations, over two directions and two frequencies, and is therefore called '4D-QTF' [28]. The second-order drift loads resulting from both QTF versions are described in Eq. 2.

$$F_{LF,2D}^{(2)} = \text{Re} \sum_i \sum_j \left[\zeta_i \cdot \zeta_j \cdot QTF_{ij} \cdot \exp(i\{(\omega_i - \omega_j)t + \varepsilon_i - \varepsilon_j\}) \right] \quad \text{Eq. 2}$$

$$F_{LF,4D}^{(2)} = \text{Re} \sum_i \sum_j \sum_k \sum_l \left[\zeta_{ik} \cdot \zeta_{jl} \cdot QTF_{ijkl} \cdot \exp(i\{(\omega_{ik} - \omega_{jl})t + \varepsilon_{ik} - \varepsilon_{jl}\}) \right]$$

The 2D-QTF is commonly applied, because this leads to conservative drift loads in deep water. It was shown that the contribution of the directional interactions to the wave drift loads is large in shallow water [28], which was the incentive for the development of the 4D-QTF. The implementation of the 4D-QTF in the method aNySIM [19] is under development as part of JIP-HAWAII. Both QTF types can be decomposed into one part consisting of the quadratic products of first-order wave contributions (QTF-I to IV), and another contributed by the second-order bound velocity potential (QTF-V).

2.4.2 Limitations of standard diffraction methods in shallow water

Standard diffraction codes are generally suitable for a large range of wave conditions in deep, open water. They assume a primary wave climate that is stationary in time and uniform in space. Interactions of this spectrum with the shore, bathymetry or obstacles are not taken into account, and the secondary wave drift loads are found using the 2D-QTF. LF free waves are

neglected and the directional spreading of LF waves is underestimated in this standard approach. Both simplifications can lead to a substantial under-estimation of the vessel response in shallow water [5][7][28], because nearshore LF wave fields can be very energetic and can have a high directional spreading. Furthermore, these QTF methods also assume an equilibrium between primary wave forcing and bound LF waves, over an infinitely long flat bottom. In shallow water, bound waves generally do not have the time to develop this equilibrium solution. While the omission of free LF waves may lead to an underestimation of LF wave loads, the equilibrium assumption for bound waves may lead to an overestimation of LF wave loads. Using the 4D-QTF instead of the 2D-QTF solves the problem of the higher directional spreading in nearshore areas; it includes the interactions between primary waves in different directions. The other problem that needs to be solved is the inclusion of LF free waves. This study aims to include a substantiated estimate of the LF free reflected wave distribution in shallow water in a vessel motion response calculation.

3 APPROACH

The general approach during this study was to create an artificial wave field from a predefined 2D wave spectrum, and then generate time series of this wave field at a number of 'sensor' locations. These time traces were then used as input for different wave analysis methods, which attempted to reconstruct the initial wave spectrum. When a suitable method for the analysis of shallow-water 2D wave fields was found, its output was used to estimate the motions of a representative nearshore moored LNGC. All of this is explained in more detail later.

3.1 Assumptions

Based on typical nearshore LNGC mooring locations, the following assumptions and boundary conditions were used throughout this study:

- An LNG terminal is located at approximately 15-40m water depth [8], on a gentle slope to a non-uniform or uniform shore;
- The frequency range of LF waves is defined between 0.03 - 0.3rad/s (alternatively 0.005 - 0.05Hz, periods between 20 - 200s), as in [8][12][13];
- The expected wave conditions include the following contributions:
 - Primary waves in incident direction approaching the coast, with a standard JONSWAP spectral shape, $T_{peak} = 13s$ and a cosine-2s DSF (e.g. [18]);
 - Corresponding directional LF bound waves in dominantly incident direction;
 - LF free waves in dominantly reflected direction, with a frequency distribution similar to that of the bound incident waves and a slightly broader cosine-2s DSF.
- The eigenfrequencies of the horizontal motions of a typical LNGC in combination with its mooring system are in this LF wave range [7].

¹The components in a short-crested wave field have directional spreading, the components in a long-crested wave field travel in (approximately) the same direction

3.2 Validity of the 2D methods

The validity of the free wave assumption that is included in all 2D wave spectrum analysis tools for different water depths should be evaluated before an attempt can be made at applying tools with this assumption to LF shallow-water wave fields. This is evaluated first in 1D using a 1D wave analysis tool that is able to separate bound and free components, as well as incident and bound components [1]. Two versions of this tool are used to analyze artificial LF wave fields in 1D: the original version and a modified version with free wave assumption. The results are compared, to separate the error introduced by the free wave assumption from possible general analysis errors. Based on this 1D analysis we concluded that the error introduced by the free wave assumption in 1D is sufficiently low to justify an attempt to apply 2D wave analysis methods with free wave assumption to LF 2D wave fields, over the considered water depth (15-40 m) and frequency domain (0.03 - 0.3rad/s).

3.3 Selected methods

2D wave analysis is conducted using three conventional directional wave analysis tools, all assuming free waves only: the efficient stochastic Extended Maximum Entropy Principle method (EMEP [11]), the flexible stochastic Bayesian Directional Method (BDM [10]) and the deterministic Rotational Directional Phase-Resolving Analysis (r-DPRA [5]).

Maximum entropy methods are based on the idea that a DSF (Section 2.2) is similar to a probability density function (PDF), since they both have an integral equal to one over all directions respectively possibilities and are both positive functions over their whole domain. A DSF can even be seen as a PDF over possible directions. The principle of the maximum entropy methods like EMEP is that an 'entropy' function is defined, which is maximized taking into account the relations given by the cross-spectra obtained from wave data.

In the BDM, the directional range is sub-divided into p ranges of width $\Delta\theta = 2\pi/p$. Over each of these sub-segments, the DSF is assumed to be constant. This means that the BDM estimate of the DSF can be written as a series of p values x_p , where the value of x_p is defined by the logarithm of the constant value of the DSF over segment p .

EMEP has a higher error tolerance than the other two methods, which might be beneficial in dealing with the error introduced by the free wave assumption if this method is applied to LF wave fields. BDM does not assume a DSF shape *a priori*, which makes this method very flexible for wave fields with multiple directional peaks.

The r-DPRA method is a deterministic wave analysis method, which uses a least-squares solution scheme to distinguish between wave directions present in a wave field. It is a recently developed in-house tool of Deltares for analysis of primary waves. This method is phase-resolving, which might have some benefits over stochastic models when its output is used in a vessel motion calculation. Another reason why this method is included in this comparison is that such a phase-

resolving method will be more easy to extend with a bound wave assumption, should we conclude that this will be necessary. A drawback of such a deterministic method is that it is expected to be more sensitive to "errors" in the input signals than stochastic methods. Since in this application r-DPRA will be used outside the range it was designed for, results may show a strong dependence on the quality of the input signals. r-DPRA was originally designed to detect main wave directions only. A post-processing extension to the original code was therefore included for this study, where the directional spreading is estimated based on the total spectral energy per frequency and the analysis resolution.

3.4 Analysis steps

The performance of the three selected 2D wave analysis methods for application to typical LF wave fields is evaluated, by using artificially generated wave fields. The aim of these analyses is to evaluate whether these 2D wave analysis methods are suitable for analysis of LF wave fields in water depths between 15 and 40m.

If one of these three methods is proven to be suitable for the determination of the directional spectrum of LF wave fields in shallow water (objective 1), the next step is to evaluate whether output from this method forms suitable input for a first estimate of the vessel response (objective 2). This second step is included in this study because a vessel acts as a filter for wave elevation; even if the estimation of the input spectrum is not perfect, it might still provide a good estimate of the most important motions of the vessel. The response of a standard, jetty-moored LNG carrier in 15m and 40m water depth to a representative wave field is evaluated.

In the overview below, these steps are summarized. Steps 1 and 2 in this overview are used to reach objective 1, steps 3 and 4 form a first step towards reaching objective 2 of this study.

- 1 Compare the performance of the three methods EMEP, BDM and r-DPRA for different artificial input wave signals.
- 2 Select the most suitable 2D method for analysis of a realistic shallow-water wave field.
- 3 Use this most suitable method to generate input for a vessel motion calculation: calculate the response of an example LNGC in a representative wave field.
- 4 Compare this response with the results from a reference response calculation using the exact input spectra and with a standard deep-water calculation. The wave analysis method should be able to approach the reference results.

The artificial input signals in both 1D and 2D are increased in complexity if the wave analyses were successful, up to realistic wave field.

The general approach used in all wave analyses is illustrated in Figure 6. An artificially generated input spectrum is used to generate time series of the wave field at predefined probe locations. These time series serve as input for three 2D

wave analysis methods. Their output spectra are subsequently compared with the input spectrum.

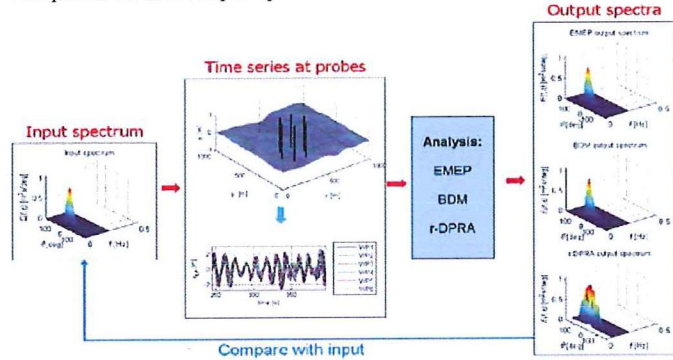


Figure 6 2D wave analysis procedure

4 2D WAVE ANALYSIS RESULTS

Since it was concluded that the free wave assumption is acceptable in 1D, the considered analysis methods were applied to 2D wave fields. 2D wave analysis was conducted using the three conventional directional wave analysis tools EMEP, BDM and r-DPRA, all assuming free waves only. Their performance for application to three types of input wave field was evaluated: primary waves (WF) only, bound waves only and a combination of bound and LF free waves. The LF wave field including bound and LF free reflected waves is the most relevant in the context of this study, because it resembles a typical shallow-water LF wave field.

A few carefully chosen spectral values were selected for a decent and concise comparison of the output and input spectra:

- Root-mean-square wave height H_{rms} [m], which is a measure for the energy content in the wave field;
- Weighed mean period T_{m01} [s], called T_{mean} here;
- Dominant direction θ_{dom} [deg], defined as the direction with the highest energy in the directional spectrum;
- Spectral width σ_s [deg], which is defined as the standard deviation w.r.t. θ_{dom} (Figure 7).

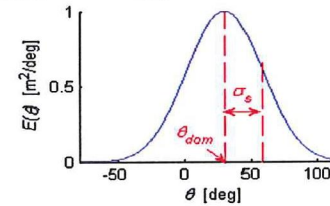


Figure 7 Dominant direction and spectral width of DSF

4.1 Analysis of benchmark WF primary 2D wave fields

All three methods deliver accurate results for a systematic variation of 2D WF primary wave fields. Important to note is that the results of all three methods are sensitive for the layout of the wave probe array and the measurement duration. The results of BDM and EMEP are comparable. r-DPRA overestimates the directional spreading of most spectra, due to assumptions that have been made in post-processing (Section 3.3). It was concluded that EMEP is not suitable for very narrow directional distributions and that EMEP and BDM are able to analyze all types of bimodal cases with two distinct

peaks, while r-DPRA is less suitable for such input spectra. No indication was found that the performance of these three methods for analysis of primary wave fields depends on water depth, spectral shape or spectral energy content.

4.2 Analysis of bound 2D wave fields

In order to test how accurately the three considered methods can resolve bound waves, the next step was to generate an artificial bound wave field, which corresponds to the benchmark primary wave spectrum. The short-crested bound wave formulation of Herbers *et al.* [12], in the implementation of Van Dongeren *et al.* [25], was applied. Time series of these bound waves only were generated at the probe locations. The radius of the probe array was optimized for λ_{bound} .

Results from all three methods for these wave fields consisting of bound waves only depend heavily on water depth over wavelength ratio h/λ , which in turn influences c_{bound}/c_{free} . All three considered methods are usable without too many restrictions for directional analysis of bound waves in shallow waters, with h/λ_{bound} below 0.04. Deeper waters (h/λ_{bound} up to 0.1) should be treated with caution. Especially BDM is unsuitable for these higher water depths (Figure 9). The shallowest water in this figure corresponds to $h = 1$ m and $\lambda_{bound} = 155$ m and the deepest water to $h = 57$ m and $\lambda_{bound} = 597$ m.

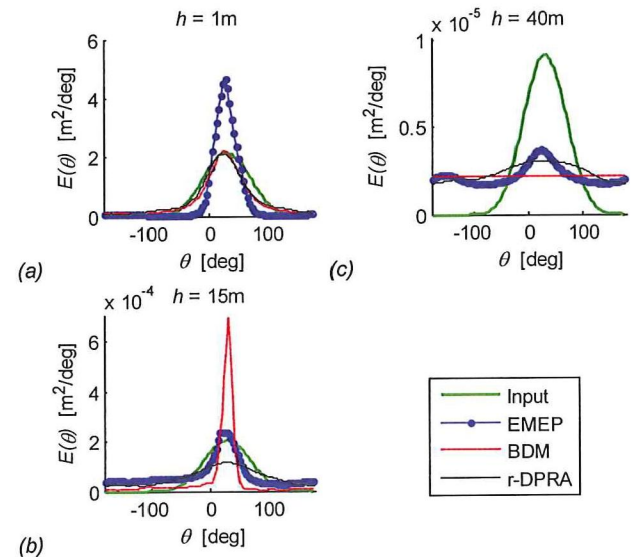


Figure 8 Input and analysis directional spectra of bound waves only at $h = 1$ m (a), 15m (b) and 40m (c)

The velocity ratio c_{bound}/c_{free} determines the performance of the methods if bound waves are present; it determines the amount of error introduced by these bound waves. This means that methods with free wave assumption not only perform well for shallow water, but also for low frequencies (analogously to 1D) and a narrow directional spreading (Figure 5).

These sensitivities were tested by varying the peak frequency and the directional spreading of the benchmark

primary spectrum separately, which influenced the frequency and the directional spreading of the bound waves and with it the performance of all three wave analysis methods. The error introduced by the free wave assumption in all three methods is distributed evenly over all directions, leading to a uniformly distributed fraction of the wave energy in the analysis results.

This uniformly distributed error increases quadratically with increasing water depth (Figure 8). EMEP and r-DPRA deliver some promising results for analysis of bound waves only.

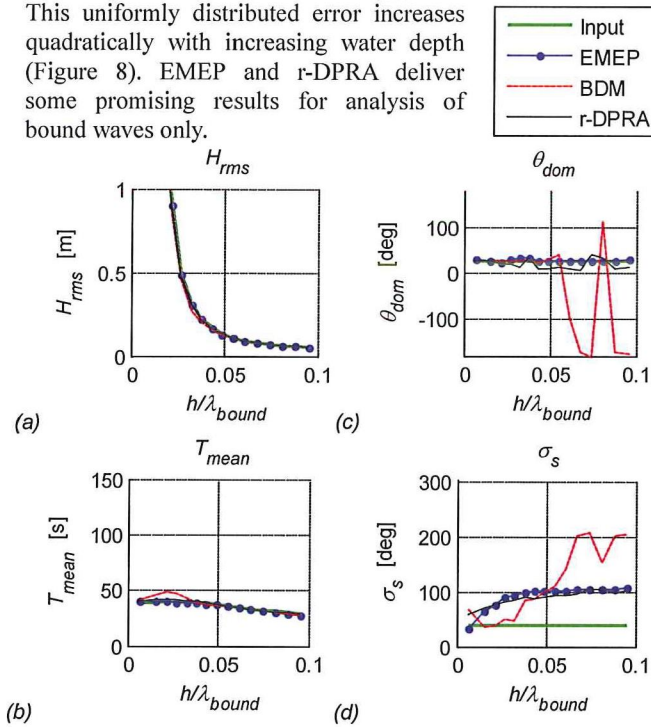


Figure 9 Sensitivity of bound wave analysis results for water depth – wave height (a), mean period (b), dominant direction (c) and spectral width (d) of input and analysis results

4.3 Analysis of 2D wave fields consisting of bound and LF free components

Subsequently, an artificially generated wave field consisting of both bound waves and LF free waves is used as input for the three analysis methods. The bound waves are the same as in the wave field consisting of bound waves only (Section 4.2). The frequency distribution of the LF free reflected waves was chosen similar to the bound frequency distribution, since LF free reflected waves primarily originate from reflected bound waves, Section 2.1. Its directional distribution is chosen similar to the primary cosine-2s spectral shape, but with a higher directional spreading. A reflection coefficient of 0.75 was assumed for all water depths.

Results show that r-DPRA is unable to detect the correct wave components and BDM only finds the dominant incident directional peak (not the secondary) for this type of wave field in very shallow water. For relatively deep water, both r-DPRA and BDM prove to be unsuitable (Figure 10). It should be noted that θ_{dom} and σ_s are less meaningful for situations with multiple directional peaks, but the deviations from the input in the figure

are not due to this effect. EMEP finds an acceptable estimate of the energy content and spectral shape of these wave fields for all considered conditions, although it deteriorates slightly towards deeper water.

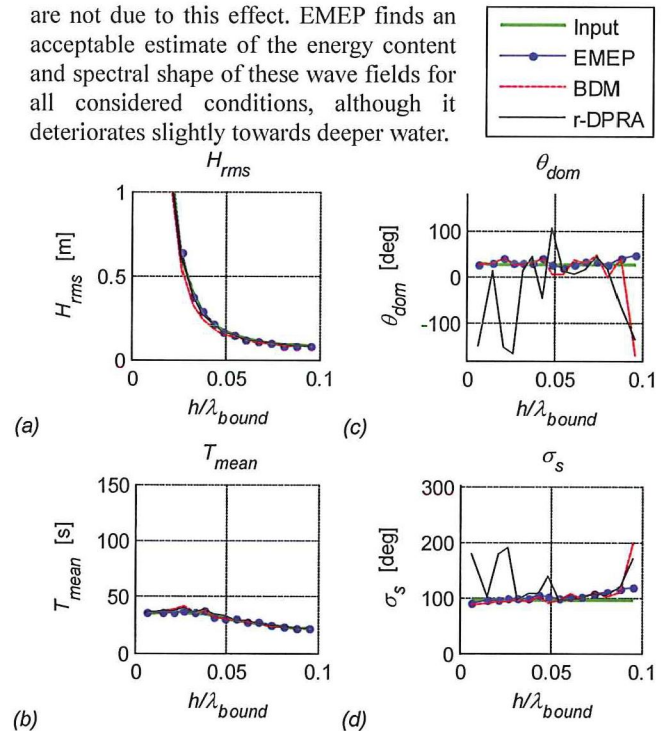


Figure 10 Sensitivity of bound plus LF free wave analysis results for water depth - wave height (a), mean period (b), dominant direction (c) and spectral width (d) of input and analysis results

The reasonable performance of EMEP can probably be attributed to its high input error tolerance. It can be concluded that EMEP is the most suitable method of the three considered methods for the determination of the directional spectrum of LF wave fields.

The influence of variation in phase seed and in the reflection coefficient of LF waves were also evaluated for these input spectra. These influences were limited, which is not further elaborated here.

4.4 Conclusions 2D wave analysis

In general, it can be concluded that EMEP is a robust method that finds a stable solution that approximates the spectral shape and energy content reasonably accurate for all considered wave fields over the project water depth and frequency domain. BDM delivers comparable results for some input fields, but it has a tendency to instability and to underestimate the secondary spectral peak (if two peaks are present). This method is only suitable in very shallow water if bound waves are present. The deterministic approach of r-DPRA makes this method the most sensitive to inconsistencies in the input. Furthermore, the applied post-processing results in a consistent overestimation of directional spreading in all wave fields. This method is in its present form unsuitable for the combination of bound and LF free reflected waves; it does not

perform well for all spectra with a high directional spreading and multiple spectral peaks.

The most important conclusion drawn from all 2D wave analyses is that EMEP is the most suitable method of the three considered methods for the determination of the directional spectrum of LF wave fields.

5 VESSEL MOTION RESPONSE CALCULATION

The identification of EMEP as the most suitable method for analysis of the directional spectrum of LF wave fields, led to the choice of this method to provide the input for a vessel motion response calculation in a representative shallow-water 2D wave field. The response of a standard, jetty-moored LNG carrier in head waves was evaluated for water depths of 15m and 40m (Figure 11). The horizontal motions surge, sway and yaw are most affected by LF loads, therefore these motions are of most interest here. The natural periods of the mooring system are 172s (surge), 274s (sway and 98s (yaw).

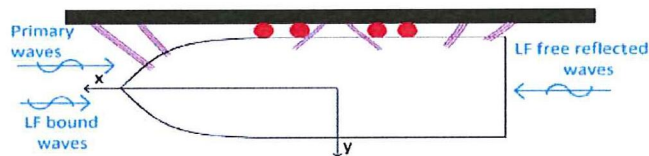


Figure 11 Direction of vessel and dominant directions of incoming waves (with spreading around these dominant directions)

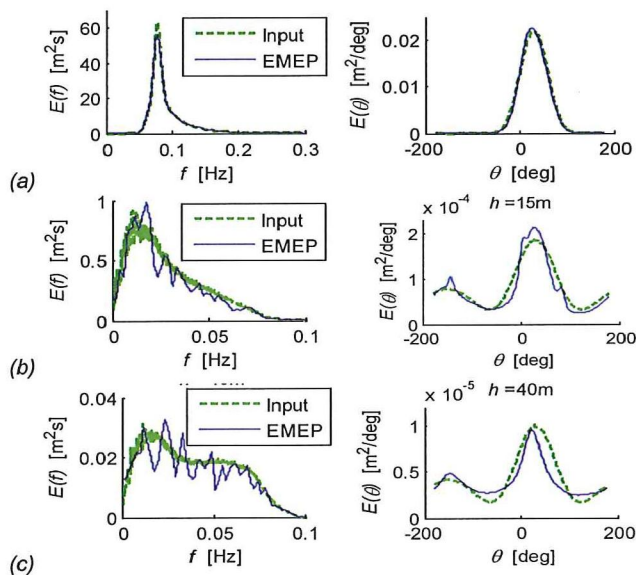


Figure 12 Input frequency (left) and directional (right) spectra and EMEP estimates – primary at 15 and 40m (a), total LF at 15m (b) and total LF at 40m (c)

This evaluation was performed for an artificially generated representative 2D wave field, consisting of a short-crested primary wave field, the corresponding short-crested bound incident wave distribution and an LF free reflected wave

distribution. The wave spectra estimated with EMEP are used as input to compute the vessel response. The input spectra and EMEP estimates that are used as input are shown in Figure 12.

The computed vessel motions were compared to a reference case in which the response was calculated using the exact input wave spectra and the total 4D-QTFs. The computed loads on the vessel and the response of the vessel are compared to the exact results in spectral sense, because phase information of the input wave components is lost in the EMEP estimate. It was investigated for the standard 2D-QTF deep-water approach that variation of the input wave seed does not have a large influence on the vessel motion spectra.

Because the bound waves are treated as if they are free in the EMEP wave analysis, their effect is now included in the total LF wave spectrum, as well as in the 4D-QTF contribution V. This means that two options are available to avoid taking the bound waves into account twice in the load calculation: either the bound interaction contribution V should be deleted from the 4D-QTF or the bound waves should be deleted from the estimated LF spectrum. Since the second option requires bound/free wave distinction, which is not straightforward, the first option is preferred. Unfortunately, the 4D-QTF-I to IV contributions could not be generated separately within the available time of this study. A very rough approximation of bound/free distinction was therefore applied to the LF wave spectrum estimate from EMEP: it was assumed that all energy in the estimated LF wave spectrum traveling in incident direction is bound (dominant WF primary wave direction $\pm 90^\circ$), and that all other LF wave energy is contributed by LF free waves. The bound waves were then excluded from the estimated LF wave spectrum by setting all incident LF wave energy to zero. This results in an estimate of the LF free wave spectrum, which can be included in the vessel response calculation separately as free waves. The total loads on the vessel resulting from this exercise are shown in Table 1, the total motions in Table 2.

Table 1 Total load m_0 estimates using the exact spectra and those estimated with EMEP as input*

Total load m_0 est.	surge	sway	heave	roll	pitch	yaw
15m -Exact	5.4E+6	1.6E+7	1.4E+8	1.1E+9	1.1E+12	1.7E+11
15m -EMEP est.	5.5E+6	2.0E+7	1.5E+8	1.1E+9	1.0E+12	1.6E+11
15m -EMEP/exact	+2%	+27%	+8%	+1%	-5%	-8%
40m -Exact	6.7E+6	1.9E+7	1.2E+8	3.3E+8	1.8E+12	1.9E+11
40m -EMEP est.	6.4E+6	1.9E+7	1.2E+8	3.1E+8	1.9E+12	1.7E+11
40m -EMEP/exact	-4%	+1%	-3%	-7%	+3%	-7%

The total loads show differences in the order of 5% for both water depths. The largest difference in this table (sway load at 15m) is caused by WF phenomena, while sway motions are dominated by LF loads (as illustrated in Figure 13). The differences in the peaks of the WF part of this sway load

spectrum are caused by the fact that EMEP estimates different directional distributions for different frequencies, even though the total directional distribution is analyzed accurately. In the LF part of the load spectrum, the EMEP estimate is very close to the exact spectrum. The sway motion is therefore predicted accurately at this water depth (Table 2).

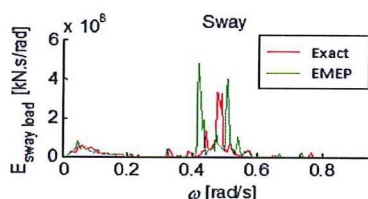


Figure 13 Total sway load spectrum at $h = 15\text{m}$ (exact & EMEP estimate)

Table 2 Total motion m_0 estimates using the exact spectra and those estimated with EMEP as input*

Total motion m_0 est.	surge	sway	heave	roll	pitch	yaw
15m -Exact	1.070	0.900	0.017	0.769	0.044	0.258
15m -EMEP est.	1.030	0.898	0.018	0.736	0.041	0.258
15m - EMEP/exact	-4%	+0%	+6%	-4%	-8%	+0%
40m -Exact	0.220	0.341	0.019	0.380	0.098	0.168
40m -EMEP est.	0.204	0.374	0.018	0.304	0.102	0.185
40m -EMEP /exact	-7%	+10%	-3%	-20%	+4%	+10%

*Legend: orange = over-estimation ($> 10\%$), red = under-estimation ($< -10\%$), green = accurate estimation (between -10% and 10%)

The response of the vessel due to the wave spectra estimated with EMEP was similar to the response resulting from the exact wave spectra. The most relevant total motions (surge, sway, yaw) show differences between the estimated and the exact motion spectra in the order of 5% at 15m, and 10% at 40m water depth (Table 2).

Because the natural frequencies of the moored LNGC are low, the loads due to the LF waves only ('LF loads') are the most relevant. The EMEP estimate of these loads is also compared to the LF loads from the reference case (Table 3).

Table 3 LF total load m_0 estimates using the exact spectra and those estimated with EMEP as input – legend see Table 1

LF load m_0 est.	surge	sway	heave	yaw
15m -Exact	2.2E+5	4.5E+6	4.8E+7	7.3E+9
15m -EMEP est.	2.4E+5	4.7E+6	4.9E+7	8.4E+9
15m -EMEP/exact	+7%	+4%	+2%	+15%
40m -Exact	3.9E+3	2.2E+4	1.1E+6	5.0E+9
40m -EMEP est.	5.2E+3	2.3E+4	1.1E+6	5.8E+9
40m -EMEP/exact	+34%	+5%	+6%	+16%

Pitch and roll are omitted, because the WF component of these motions is dominant (the LF components are an order of magnitude smaller). LF heave is included even though it is dominated by WF waves, because it is a measure for the total LF wave level. The LF loads (including both LF free and LF

bound wave loads) were estimated by low-pass filtering the total load spectra at $\omega = 0.3\text{rad/s}$.

The agreement between the EMEP results and the reference case for LF loads is slightly better for 15m water depth than for 40m. This was expected, since the EMEP estimate of the total LF spectrum is more accurate at 15m (Figure 12). It should be noted that the LF waves and loads are very small at 40m water depth, which makes the procedure much less relevant than at 15m. In general, EMEP provides conservative LF load results. The overestimation of the yaw and sway loads at 40m can be explained by the slight overestimation of the transverse waves by EMEP. In general, it can be said that the differences in loads can be caused by the peakedness of the frequency spectrum estimated by EMEP (Figure 12). The EMEP yaw spectrum at 15m for instance shows a peak around the natural frequency of yaw (0.01Hz), which can explain the overestimation of the yaw load. These differences are limited and seed-dependent. Using additional smoothing or seed variation of the EMEP spectrum before using it as input for the response calculation could reduce the differences in loads.

The comparison of LF loads is important, because including the estimate of the LF free reflected waves is the benefit of the newly developed method: it provides a fast and efficient estimate of the free LF waves present at the mooring location. These results show that this new method delivers promising results for LF loads, especially for $h = 15\text{m}$, where the absolute energy of the LF free waves is generally high.

This approach is not perfect yet and still has some differences with the reference case, which are partly introduced by the rough estimate that all reflected LF waves are free. This could be improved further in the future, but from a practical point of view we conclude that the use of EMEP to estimate LF waves as input for a vessel response calculation delivers promising results.

A substantial part of the total LF loads is contributed by LF free waves (see Figure 14; order of 10% for $h = 15\text{m}$ and 25% for $h = 40\text{m}$).

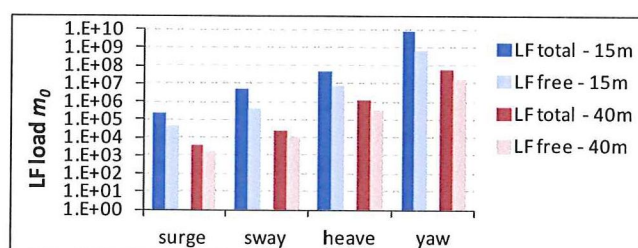


Figure 14 Fraction of the total load m_0 that is due to LF free waves with the exact input wave spectra, for the reference wave field at 15m and 40m water depth (logarithmic scale)

The influence of directionally spread LF free waves on the vessel surge response is much lower though than in case of uni-directional LF free components with the same energy and direction (this was in the order of 70% of the total linear LF

surge motion for this vessel at $h = 15\text{m}$; Jaouen *et al.* [15]). This is explainable; more energy travels in different directions than head-on the vessel. Figure 14 also shows that the total LF loads are substantially lower at 40m than at 15m.

Overall, an acceptable estimation of the vessel loads and response was found using the estimated wave spectra from EMEP as input. This conclusion has some limitations though, which lead to recommendations for further research. An important limitation is that only one wave field was evaluated, such that these results only provide a first indication. The results are very promising, but further validation is recommended. Another concern is the practical application of the results presented above. A rough approximation of the bound/free distinction was used, assuming that all incident LF waves in the total estimated LF wave spectrum with EMEP are bound. This is not generally applicable in more complex coastal areas, which requires further evaluation (see discussion).

6 CONCLUSIONS AND DISCUSSION

6.1 Conclusions

The conclusions that can be drawn are summarized below:

- 1 EMEP is the most suitable method of the considered methods to determine the directional spectrum of artificially generated LF wave fields (bound + free waves).
- 2 The computed response of an example vessel to a representative wave field using an LF wave spectrum that was estimated by EMEP as input was overall acceptable. This is the first indication that EMEP output might be suitable as input for a vessel motion evaluation. The procedure was shown to be more promising for 15m water depth than for 40m. The benefit of the EMEP analysis procedure with respect to state-of-the-art response methods is the ability to include the LF free wave distribution in a local wave field in the vessel response calculation. It was shown that this type of waves can have a substantial contribution to the total LF wave loads on a vessel in shallow water.

These conclusions show that the use of EMEP to obtain a first estimate of LF waves can be very efficient in early stages of the design of a LNG terminal. However, this approach still has some limitations that lead to recommendations for further research. This is further elaborated in the discussion.

6.2 Discussion

In general, more attention should be paid to the validation of the use of EMEP to determine the LF wave spectrum in practical situations and to the evaluation of the use of EMEP results as input for a vessel motion response calculation in general.

EMEP proved to provide very promising results for artificial signals. The method is expected to perform equally well for numerical wave models, but it is recommended to validate the use of EMEP for analysis of LF wave model results, as well as for non-uniform bathymetries.

The use of EMEP results in a vessel motion calculation requires more validation; only a first indication of this possibility for one wave field and one vessel layout was presented here. Results were very promising, but variation of the wave field and vessel configuration is recommended. The most important remaining question in this validation is how to distinguish bound and LF free components before they can be used as input for a vessel motion calculation. Alternatively, it could be investigated whether it is possible to estimate all the LF loads using 1st order load calculations applied to the total estimated LF spectrum. This would imply that the fifth (V) contribution in the 4D-QTF is replaced by straightforward 1st order RAOs. This means that the free wave assumption ('all LF waves obey the dispersion relation') is also used in the response calculation phase. The effect of this assumption on the overall response of the vessel could be evaluated to obtain a practical method.

ACKNOWLEDGEMENTS

We would like to thank Martijn de Jong from Deltares for his help and advice concerning the r-DPRA method, and Mr. Johnson from the UWA for the use of the EMEP and BDM implementations in the DIWASP toolbox [16].

REFERENCES

- [1] Bakkenes, H.J. (2002), Observation and separation of bound and free low-frequency waves in the nearshore zone, *MSc – thesis, Delft University of Technology, Delft*.
- [2] J.A. Battjes, H.J. Bakkenes, T.T. Janssen, A.R. Van Dongeren (2004), Shoaling of subharmonic gravity waves, *J. Geophys. Res.*, 109 (C02009), pp. 1–15
- [3] Benoit, M., P. Frigaard and H.A. Schäffer (1997), 'Analyzing multidirectional wave spectra: a tentative classification of available methods', *Proc IAHR-Seminar: Multidirectional Waves and their Interaction with Structures*, 10-15 August 1997, San Francisco, CA, USA, pp. 131-158.
- [4] Brillouin, L. (1960), Wave propagation and group velocity, *Academic Press*, New York.
- [5] De Jong, M.P.C., M.J.A. Borsboom and J. Dekker (2009), Calculation of low-frequency waves in shallow water and comparison to common practice in diffraction methods, *OMAE2009-79401*, 31 May - 5 June, Honolulu, Hawaii, USA.
- [6] De Jong, M.P.C. and Borsboom, M.J.A. (2012), A Practical Post-Processing Method To Obtain Wave Parameters From Phase-Resolving Wave Model Results, *International Journal of Ocean and Climate Systems*, Volume 3, Number 4, December 2012, ISSN 1759-3131
- [7] Deltares, MARIN, Bureau Veritas, SBM (2008), HAWAII JIP - Shallow water initiative WP4 – Summary report.
- [8] Deltares, MARIN, Bureau Veritas, Shell (2009), sHallow Water Initiative (Hawaii JIP) – project plan V2.0.
- [9] Elgar, S., T.H.C. Herbers, M. Okihiro, J. Oltman-Shay and R.T. Guza (1992), Observations of infragravity waves, *Journal of Geophysical Research*, 97(C10), 15573-15577.
- [10] Hashimoto, N., K. Kobune and Y. Kameyama (1987), Estimation of directional spectrum using the Bayesian approach and its application to field data analysis, *Rep. of Port and Harbor Res. Inst.*, Vol 26.
- [11] Hashimoto, N., T. Nagai and T. Asai (1994), Extension of maximum entropy principle method for directional wave

- spectrum estimation, *Proc. 24th Int. Conf. on Coastal Eng. (ASCE)*, pp. 232-246, Kobe, Japan.
- [12] Herbers, T.H.C., S. Elgar and R.T. Guza (1994), Infra-gravity frequency motions on the shelf. Part I: forced waves, *Journal of Physical Oceanography*, 24, 917-927.
 - [13] Herbers, T.H.C., S. Elgar, R.T. Guza and W.C. O'Reilly (1995-a), Infragravity-frequency (0.005-0.05Hz) motions on the shelf. Part II: free waves, *Journal of Physical Oceanography*, 25, 1063-1079.
 - [14] Holthuijsen, L.H. (2007), *Waves in Oceanic and Coastal Waters* (2nd edition, 2008), *Cambridge University Press*, Cambridge, UK, pp. 106-309.
 - [15] Jaouen, F., W. Otto and O.J. Waals (2012), Frequency domain computations of a LNGC motion response spectra (draft), *Report No. 23313-1-CPO*, MARIN.
 - [16] Johnson, D. (2001), DIWASP Directional Wave Spectra Toolbox - User Manual Version 1.3, *Centre for Water Research, University of Western Australia*, Rep. no. WP 1601 DJ.
 - [17] Longuet – Higgins, M.S. and R.W. Stewart (1962), Radiation stress and mass transport in gravity waves, with application to 'surf beats', *Journal of Fluid Mechanics*, 13, 481-504.
 - [18] Longuet-Higgins, M.S., D.E. Cartwright and N.D. Smith (1963), Observations of the directional spectrum of sea waves using the motions of a floating buoy, *Ocean wave spectra*, New York, Prentice Hall, pp. 111-136.
 - [19] Maritime Research Institute Netherlands, aNySIM product leaflet (2010) - time domain analysis of multi body dynamics for offshore operations.
 - [20] Munk, W.H. (1949), Surf beats, *Eos Trans. Amer. Geophys. Union*, 30, pp. 849-854.
 - [21] Pierson, W.J., G. Neumann and R.W. James (1955), Practical methods for observing and forecasting ocean waves by means of wave spectra and statistics, *US Navy Hydrographic Office Pub.*, 603
 - [22] Pinkster, J.A. (1980), Low frequency second order wave exciting forces on floating structures, *PhD thesis*, Delft University of Technology, Delft, The Netherlands.
 - [23] Roelvink, D., A.J.H.M. Reniers, A.R. van Dongeren, J. van Thiel de Vries, R. McCall and J. Lescinski (2009), Modeling storm impacts on beaches, dunes and barrier islands, *Journal of Coastal Engineering*, doi: 10.1016/j.coastaleng.2009.08.006.
 - [24] Tucker, M.J. (1950), Surf beats: sea waves of 1 to 5 minute period, *Proc. Royal Society London, Ser. A*, 202, 565-573.
 - [25] Van Dongeren, A.R., A.J.H.M. Reniers, J.A. Battjes and I. Svendsen (2003), Numerical modeling of infragravity waves response during DELILAH, *Journal of Geophysical Research*, 108(C9), 3288, doi:10.1029/2002JC001332.
 - [26] Voogt, A, T. Bunnik and R.H.M. Huijsmans (2005), Validation of an analytical method to calculate wave setdown on current, *OMAE-2005-67436*, 12-17 June 2005, Halkidiki, Greece.
 - [27] Waals, O.J. (2009-a), On the application of advanced wave analysis in shallow water model testing (wave splitting), *OMAE2009-79413*, 31 May - 5 June, Honolulu, Hawaii, USA.
 - [28] Waals, O.J. (2009-b), The effect of wave directionality on low frequency motions and mooring forces, *OMAE2009-79412*, 31 May - 5 June, Honolulu, Hawaii, USA.

